

Spring 5-2017

## Characterization of Epoxy/Amine Networks with Glycidal Polyhedral Oligomeric Silsesquioxane Surface Modified Silica Nanoparticles

Reese K. Sloan  
*University of Southern Mississippi*

Follow this and additional works at: [https://aquila.usm.edu/honors\\_theses](https://aquila.usm.edu/honors_theses)

 Part of the [Polymer Chemistry Commons](#)

---

### Recommended Citation

Sloan, Reese K., "Characterization of Epoxy/Amine Networks with Glycidal Polyhedral Oligomeric Silsesquioxane Surface Modified Silica Nanoparticles" (2017). *Honors Theses*. 491.  
[https://aquila.usm.edu/honors\\_theses/491](https://aquila.usm.edu/honors_theses/491)

This Honors College Thesis is brought to you for free and open access by the Honors College at The Aquila Digital Community. It has been accepted for inclusion in Honors Theses by an authorized administrator of The Aquila Digital Community. For more information, please contact [Joshua.Cromwell@usm.edu](mailto:Joshua.Cromwell@usm.edu), [Jennie.Vance@usm.edu](mailto:Jennie.Vance@usm.edu).

The University of Southern Mississippi

Characterization of Epoxy/Amine Networks with Glycidal Polyhedral Oligomeric  
Silsesquioxane Surface Modified Silica Nanoparticles

by

Reese Keeling Sloan

A Thesis  
Submitted to the Honors College of  
The University of Southern Mississippi  
in Partial Fulfillment  
of the Requirement for the Degree of  
Bachelor of Science  
in the Department of Polymer Science

May 2017



Approved by

---

Jeffrey Wiggins, Ph. D., Thesis Advisor  
Associate Professor of the School of Polymers

---

Jeffrey Wiggins, Ph.D., Director  
Department of Polymers and High Performance Materials

---

Ellen Weinauer, Ph.D., Dean  
Honors College

## Abstract

Silica nanoparticles were surface modified with octa-functional glycidal polyhedral oligomeric silsesquioxane (G-POSS) and incorporated into an epoxy/amine system in an effort to increase the mechanical performance of the inorganic/organic hybrid material. The silica nanoparticles were first functionalized with 3-aminopropyltrimethoxysilane (APTMO) at 5 and 10 weight percent, and then modified with G-POSS at ratios of 1:10 and 1:5 (APTMO: G-POSS). The modified particles were then incorporated into an epoxy/amine network consisting of diglycidyl ether of bisphenol A (DGEBA) and aromatic amine, diamine diphenyl sulfone (4,4' DDS) at 1 and 5 weight percent, resulting in 8 different formulations. The incorporation of the modified silica nanoparticles caused changes in crosslink density depending on the amount functionalization density, G-POSS modification, and loading. Samples with nanoparticles of higher functionalization density and lower G-POSS modification exhibited higher crosslink density due to high functionalization and lower free volume. It was determined that incorporation of inorganic POSS cage disrupted network formation and chain packing. Similar trends follow suite with the strength of the material in compressive analysis. The incorporation of the nanoparticles slightly decreased the gel point of the material as compared to that of the control. Furthermore, it was determined that there is an optimum degree of modification and loading that would influence the mechanical properties and performance of the material to its optimal values.

Key words: Epoxy/amine, thermoset, network formation, POSS, free volume

## **Dedication**

To my parents, Richard and Lucinda, for their unwavering love and support throughout  
my academic career.

## **Acknowledgements**

I would like to thank my advisor, Dr. Jeffrey Wiggins, for his support and advice throughout this project and my career at the University of Southern Mississippi. I would not be at the point in my career where I am today if it were not for his guidance. Thank you for everything.

I would also like to thank Amit Sharma, for his input, guidance, and patience throughout my research. I would also like to thank the entirety of the Wiggins Research Group for their input and encouragement throughout my research. I honestly cannot thank all of you enough.

## Table of Contents

List of Tables.....	ix
List of Figures .....	x
List of Abbreviations .....	xi
Chapter 1: Introduction .....	1
1.1 Thermosets .....	2
1.2 Rheology of Thermosetting Networks .....	3
1.3 Functionalization of Silica Nanoparticles .....	4
1.4 POSS .....	6
1.5 Nanocomposite Material Characterization .....	8
Chapter 2: Experimental Methods .....	10
2.1 Materials .....	10
2.2 Preparation of G-POSS/silica Nanoparticle Materials .....	10
2.3 Preparation of Epoxy/amine Nanocomposite Materials .....	11
2.4 Dynamic Mechanical Analysis (DMA) of the Epoxy/amine Nanocomposite Material .....	12
2.5 Compression Testing of the Epoxy/amine Nanocomposite Materials .....	13
2.6 Rheological Testing of the Epoxy/amine Nanocomposite Materials.....	13
2.7 Scanning Electron Microscopy (SEM) of the Epoxy/amine Nanocomposite Material.....	13
Chapter 3: Results and Discussion .....	13
3.1 Dynamic Mechanical Analysis .....	13
3.2 Compression Analysis of Epoxy/amine Nanocomposite Materials.....	16



3.3 Rheological Analysis of Epoxy/amine Nanocomposite Materials.....	19
3.4 Scanning Electron Microscopy of the Epoxy/amine Nanocomposite Materials .....	21
Chapter 4: Conclusion .....	24
Chapter 5: Future Work .....	26
References.....	28

## **List of Tables**

Table 1: Sample names and sample status.....	12
Table 2: Crosslink density and average Mw between crosslinks.....	14
Table 3: Glass transition temperatures.....	16
Table 4: Average moduli, yield stress, and yield strain.....	17
Table 5: Sample gel points, initial viscosities, and lower level viscosities.....	20

## List of Figures

Figure 1: Depiction of the chemical structure of DGEBA and 4,4 DDS.....	2
Figure 2: Depiction of silica nanoparticle surface functionalization with 3-aminopropyltrimethoxysilane.....	5
Figure 3: Typical structure of a G-POSS molecule.....	6
Figure 4: General compressive analysis of tested samples to the control.....	18
Figure 5: Storage and loss modulus crossover of ‘10%-1:10-5%’ during cure process...	19
Figure 6: Complex viscosity of ‘10%-1:10-5%’ during cure process.....	20
Figure 7: Sample 10%-1:10-1%, sample 10%-1:10-5%, and sample 10%-1:5-1% under SEM.....	22
Figure 8: Sample 10%-1:5-1% under SEM at different magnifications.....	23
Figure 9: Sample 5%-1:10-1%, sample 5%-1:10-5%, sample 5%-1:5-1%, and sample 5%-1:5-5% under SEM.....	24

## **List of Abbreviations**

DGEBA – Diglycidal ether of bisphenol A

4,4 DDS – 4,4 Diamine diphenyl sulphone

APTMOs – 3-aminopropyltrimethoxysilane

G-POSS – Glycidyl Polyhedral Oligomeric Silsesquioxane

MPS – Mesoporous Silica

DMA – Dynamic Mechanical Analysis

SEM – Scanning Electron Microscopy

## **Chapter 1: Introduction and Literature Review**

Engineers are constantly attempting to find ways to improve their products. In particular, the automobile and aerospace industries are constantly looking to make their products more cost effective and desirable to the consumer. These aspects can be met by increasing the fuel efficiency of the automobile or aircraft. In order to increase fuel efficiency, the weight of the automobile or aircraft must be reduced. One of the prominent ways to reduce the weight of automobiles and aircrafts is to use composite materials as the material of construction.

A composite material is made up of two or more different materials, in order to strengthen the overall product while lowering the weight. It is typically made up of a matrix material and a reinforcing agent. The matrix is designed to house the reinforcing agent, which in return gives added mechanical benefits.<sup>1,2</sup> Composite materials often exhibit high strength to weight ratios. This property of composite materials is highly desired by manufacturers, due to the ability of composite materials to replace heavy, bulky metal parts. However, since composite materials are used to replace materials that are currently in use, they must be able to withstand the forces that are commonly present for these materials. For example, materials in the aerospace industry undergo intense forces of flight, atmospheric radiation, and atmospheric moisture. Therefore, a material engineer would have to select a polymeric matrix and reinforcing agent that would be able to withstand these variables along with providing a higher strength to weight ratio. However, a problem facing composite materials is that the polymeric matrix of the material will fail before the maximum mechanical properties of the reinforcing agent is

ever realized. Therefore, there is always a need to identify new matrix materials to improve the performance of existing ones.

### 1.1 Thermosets:

Thermosets are characterized by their highly intricate crosslinking networks.<sup>3</sup> These networks provide mechanical properties that are not provided by thermoplastic materials, such as high modulus and thermal stability. Thermosets, unlike their thermoplastic counterparts, do not melt in the presence of heat. However, heat can cause these types of materials to degrade. These crosslinking networks also provide material with large amounts of strength.<sup>4</sup>

There are multiple types of thermosetting materials, one of which are epoxy resins. Epoxies are typically made by the chemical reaction of epichlorohydrin and bisphenol-A. This reaction causes the formation of diglycidal ether of bisphenol-A (DGEBA), a typical epoxy resin.

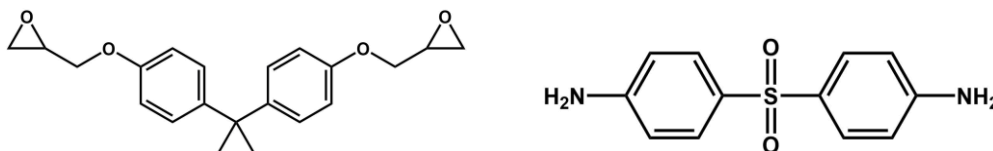


**Figure 1:** Depiction of the chemical structure of DGEBA (left) and 4,4 DDS (right)

Figure 1 shows the chemical structure of DGEBA. A curative can then be added to DGEBA to induce a crosslinking network. A common curative that is used is a diamine. These diamines are used due to their high reactivity with the epoxide functional group.<sup>5</sup> Figure 1 depicts the chemical structure of 4,4-DDS, which is a common aromatic amine curative for epoxy resins in the aerospace industry. Since both the DGEBA and diamine monomers have an average functionality that are greater than two, a crosslinking network is able to be produced.

Due to the desired mechanical properties of epoxy/amine thermosetting materials, they have become a common choice for matrix materials in composite and nanocomposite products.<sup>4,5</sup> Depending on the functionalities of the two monomers, different crosslinking effects can be manufactured by the experimenter.

## **1.2 Rheology of Thermosetting Networks:**

One of the most distinguishing characteristics of thermosetting materials is their ability to form crosslinking networks. Crosslinking networks are established by the introduction of a curing agent, which in turn cause a viscous liquid material to turn into a hard, heat and solvent resistant solid material. This transformation is irreversible.<sup>4,6</sup> The point at which the material loses all fluidity and forms a permanent shape is known as gelation or the gel point. This point of gelation can also be defined as the point in which the weight average molecular weight diverges to infinity.<sup>4,6,7</sup> This event is characterized by a dramatic increase in viscosity and the development of elastic qualities, which have otherwise not been present. Beyond the gel point, the polymeric crosslinking reaction continues to form an infinite network with increasing crosslinking density and thermal and mechanical properties. Therefore, the material can now be considered one molecule.<sup>4</sup> The curing of thermosetting materials can be classified into three stages. In stage A, the material is unreacted monomers. Stage B refers to a partially reacted system. This system typically exhibits a vitrified quality, meaning that a glassy formation has occurred, although the material is still below its gel point. However, with the introduction of heat, the glassy formation can be melted back down and processed. Stage C describes a fully cured, crosslinking network.<sup>6</sup> It is important for a material manufacturer to know the time of gelation for a material at a particular cure profile. This

is so the manufacturer will be able to process the material in the B stage of curing. The gel point of thermosetting materials is easily determined by rheological experimentation.

Another important aspect of rheology that is important to consider is the formation of networks at different cure profiles. Temperature is often used to modify the viscosity of a material in order to allow it to be more easily processed. With the use of different cure profiles for thermosetting materials, the viscosity level is needed to be determined. This is due to the fact that at the lowest level of viscosity, a material shows the greatest flow-ability due to the polymer chains of the materials being able to move freely.<sup>4</sup> This is also important to know because any added materials, such as POSS and silica nanoparticles, will have the greatest amount of mobility and ability to re-agglomerate at the material's lowest level of viscosity. However, as the polymer chains react with one another as a result of curing, the viscosity of the material will inadvertently rise. Therefore, it is important for a thermosetting material manufacturers to find the best curing methods that offer an adequate viscosity level for a desired amount of time.<sup>8</sup> This data can easily be obtained through simple rheological experimentation.

### **1.3 Functionalization of Silica Nanoparticles:**

Surface functionalized silica nanoparticles have been studied widely in epoxy networks. In-fact, there are some silica nanoparticle dispersion in epoxies commercially available.<sup>9</sup> They were first used in epoxies due to the fact that researchers were looking for additives that could increase the material's mechanical properties without dramatically increasing viscosity. Beforehand, researchers were using materials such as carboxy terminated butadiene acrylonitrile copolymers (CTBN) and core-shell polymers. These additives were shown to increase certain mechanical properties. However, when



these materials were introduced into epoxies that were designed to be cured by the introduction of a hardener or curative, they reacted in such a way that either decreased the desired mechanical properties or became insoluble in the network.<sup>9</sup> Therefore, researchers turned to the use of silica nanoparticles in the matrix material. The silica nanoparticles were dramatically smaller in size as compared to their predecessors. These nanoparticles were also able to increase mechanical properties, such as strength, modulus, stiffness, and toughness, of the overall material. Another desired quality of the silica nanoparticles was the fact the particles had a functionalized surface. Odegard et al showed that by a certain manufacturing method, silica nanoparticles can be manufactured to have a large amount of hydroxyl functional groups on their surfaces.<sup>9</sup> This offers a large advantage to material engineers for the fact that the hydroxyl groups are reactive with other functional groups to give large amounts of possibilities of surface functionalization and modification of the silica nanoparticles. One such example of this type of silica nanoparticle surface modification can be observed through the treatment of the nanoparticle with APTMOS. This type of surface modification is depicted in Figure 2.

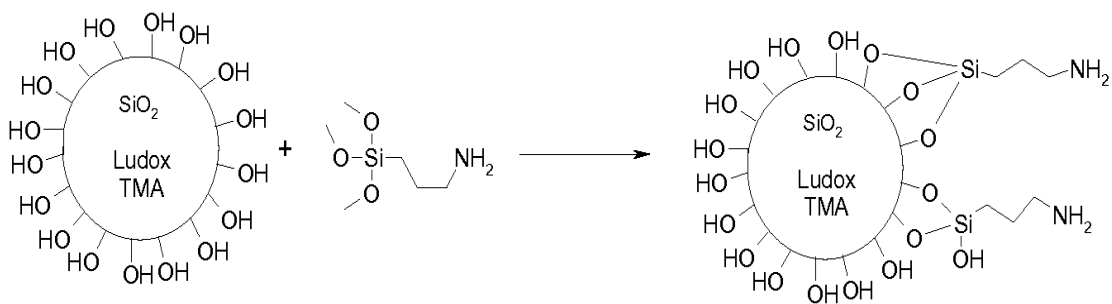


**Figure 2:** Depiction of silica nanoparticle surface modification with 3-aminopropyltrimethoxysilane<sup>10</sup>

This treatment functionalizes the surface of the silica nanoparticle with reactive amine functional groups. These functional groups are then able to be reacted with other materials present in the overall matrix material.<sup>11</sup>

#### 1.4 POSS:

Along with silica nanoparticles, other additives have been developed to provide the benefits that come with the addition of both organic and inorganic materials to the polymer matrix. By doing so, experimenters are able to increase the processability, toughness, thermal stability, and oxidative stability of materials. One such chemical is known as POSS. POSS is an inorganic-organic hybrid material made with an inorganic cage-like structure, consisting of silicon and oxygen atoms, with organic constituents extending off of the cage.<sup>12</sup> These organic substituents can be any organic functional group, such as an epoxide or inert group. POSS molecules typically have diameters ranging from 1 to 2 nanometers, therefore making it a smallest possible nanoparticle.<sup>13</sup> One specific structure of POSS is depicted in figure 4.

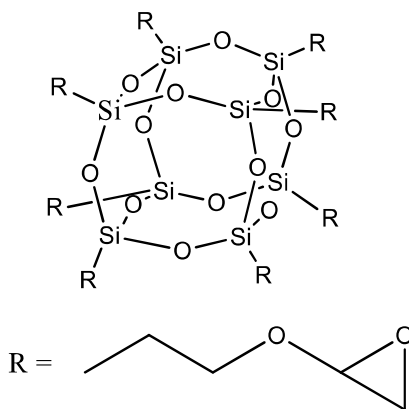


**Figure 3:** Typical structure of a G-POSS molecule

Based on the functionalities of the organic substituents, POSS has the capability of being compatible with various organic surroundings. Researchers have found that the

dispersion of POSS in a polymeric material can have great benefits to its mechanical properties, such as increased strength, modulus, and rigidity.<sup>12,13</sup> With these benefits in mind, researchers have found two different methods to incorporate POSS into polymeric materials. The first method involves the incorporation of POSS by covalently bonding the material to the polymer. The second method is based on physical blending, in which POSS molecules are not chemically linked with the polymer. This method is dependent on the compatibility of POSS molecules with the polymeric material.<sup>13</sup> However, the dispersion of POSS into certain polymeric materials is hard to achieve due to interactions between POSS molecules causing them to aggregate within polymer. Nevertheless, POSS that is introduced into an epoxy/amine network has been proven to show a significant increase the mechanical properties of the network.<sup>13,14</sup>

Researchers at the Northwestern Polytechnical University in China have recently discovered a way to increase dielectric, thermal, and mechanical properties of epoxy nanocomposites by the incorporation of mesoporous silica (MPS) and functionalized POSS.<sup>14</sup> Originally, these researchers were looking for ways to reduce the dielectric constant value of epoxy materials while also maintaining the mechanical properties of the material. It was previously known that POSS both increased mechanical properties and reduced the dielectric constant. However, large amounts of POSS are needed to show a significant decrease in the dielectric constant of the epoxy material. This amount of POSS in the epoxy material compromises the mechanical and thermal properties of the material, the opposite of what it was initially intended to accomplish.<sup>14</sup> MPS was found to have a larger pore volume and a stiffer skeleton of silica center than that of POSS. Therefore, the introduction of MPS to the epoxy material is much more suitable to

decrease the dielectric constant of the material. However, polymer material is able to penetrate the pores of MPS. This leads to a decrease in the effectivity of MPS to decrease the epoxy materials' dielectric constant.<sup>14</sup> This led researchers to find a way to incorporate both of these materials into the epoxy material. They found a way to react G-POSS, POSS molecules whose substituents are epoxide functional groups, with MPS, whose surface was modified to contain amine functional groups. Through this reaction, the G-POSS was able to encapsulate the MPS. This would prevent polymer from penetrating the pores of the MPS. As a result, the MPS would be able to reduce the dielectric constant, while the POSS would be able to increase the mechanical properties of the overall material.<sup>14</sup>

This work focuses on the ability to modify the surface of silica nanoparticles with G-POSS at varying initial functionalization densities and different G-POSS modification values. This was accomplished by systematically varying the number of amine functional groups present on the surface of the silica nanoparticles (initial functionalization), allowing for different amounts of G-POSS molecules interact with the functionalized nanoparticles. Furthermore, the amount of G-POSS present to modify the surface of the silica nanoparticles was also varied, as well as the modified nanoparticles being incorporated at different loading levels in the epoxy/amine system. Herein, the effects on the mechanical and rheological effects of the incorporation of the modified nanoparticles have on the epoxy/amine network are reported.

### **1.5 Nanocomposite Material Characterization:**

Dynamic mechanical analysis (DMA) is one of the most common methods used to characterize the thermomechanical properties of polymeric materials<sup>15</sup> The most

common form of DMA is done by taking a polymeric bar of known length, width, and height and putting it through a stress of known frequency and temperature. This is typically done to find three specific values; the storage modulus, the loss modulus, and the  $\tan \delta$ . The storage modulus corresponds to the material's elastic like component. The loss modulus represents the viscous behavior of the material. The value of  $\tan \delta$  of a material is represented by the following equation:

$$\text{Tan } \delta = \frac{\text{Loss Modulus}}{\text{Storage Modulus}}$$

This value represents the viscous component of the material over the elastic like component. This value also corresponds to the materials glass transition temperature.<sup>15</sup>

Mechanical properties of crosslinking networks are generally determined by the stress-strain behavior in compression mode.<sup>16</sup> By producing stress-strain diagrams, compressive analysis can be used to determine the modulus of a material since the  $E = \frac{\sigma}{\epsilon}$ ; where  $E$  is modulus,  $\sigma$  is stress, and  $\epsilon$  is strain.<sup>16</sup> Along with modulus, other mechanical values can be found by compressive analysis. One such variable is yield point which is best defined as the point at which a material is permanently deformed due to a force acting upon it.

SEM offers a look at the outside surface of the surface modified silica nanoparticles. This type of imaging is often used to find manufacturing inconsistencies at the microscopic level.<sup>17,18</sup> This method is helpful to develop an idea of how different molecules disperse and interact into the material, such as determining sample inhomogeneity.

## Chapter 2: Experimental Methods

### 2.1 Materials:

Silica nanoparticles, 10 nm (99.5%), were purchased from US Nano Inc. Certified reagent grade acetone ( $\geq 99.5\%$ ) was purchased from Fisher Scientific. 3-aminopropyltrimethoxysilane (APTAMOS, 95%) was purchased from Acros Organics. Ethanol (200 proof) was purchased from Decon Laboratories Inc. Glycidal Polyhedral Oligomeric Silsesquioxane (G-POSS, EP0409) was obtained from Hybrid Plastics. Diglycidal Ether of Bisphenol A (DGEBA), consisting of functional equivalent weight of 177.5 (EPON 825), was obtained from Hexion Inc. 4,4' diaminodiphenolsulphone (DDS) was purchased from ATUL sulphos. All materials were used as received.

### 2.2 Preparation of G-POSS/silica Nanoparticle Materials:

5 grams of silica nanoparticles were dispersed into an appropriate amount of ethanol (5 mg/mL of ethanol) by means of ultra-sonication for 30 minutes (2 seconds pulse on followed by 3 seconds off). Different loading levels of APTAMOS (5 and 10 wt. %) was then be added to the dispersion of silica nanoparticles to induce surface functionalization. The mixture was allowed react for 12 hours at room temperature. The functionalized silica nanoparticles were then isolated and purified by a centrifugation/re-dispersion process (10 mins at 8500 rpm, 3 times). The nanoparticles were then dried overnight at 60°C under vacuum. Each of the different surface functionalized silica nanoparticle batches were dispersed in acetone with G-POSS at two different ratios (1:10 and 1:5, APTAMOS: G-POSS). The mixture was allowed to react for 12 hours at 40°C under reflux. The surface modified silica nanoparticles were then isolated and purified

by a centrifugation/re-dispersion process (for 10 min at 8500 rotations per minute, 3 times). The nanoparticles were then dried over night at 60°C under vacuum.

### **2.3 Preparation of epoxy/amine nanocomposite material:**

Appropriate amounts of DGEBA and G-POSS modified silica nanoparticles to produce materials with 1 and 5 percent loading of nanoparticles were placed in an Erlenmeyer flask equipped with a vacuum assembly and magnetic stirbar. A small amount of acetone was added to homogenize the reactant mixture. The temperature was then ramped to 80°C with under constant stirring at 150 rpm to evaporate the solvent from the mixture. Once homogenized, the reactant mixture was then put under vacuum ( $10^{-3}$  Torr). This was continued until was properly degassed. An appropriate amount of 4,4 DDS was then added to the reaction vessel. Once the stir bar is able to move freely, the temperature will be ramped to 120°C with stirring at 150 rpm. Degassing of the reaction is restarted once the 4,4 DDS had fully dissolved into the reaction mixture. After approximately 1 hour, the material was poured into preheated silicon molds to fabricate networks, with a small portion of the uncured mixture reserved for rheological testing. The material that was poured into molds was put through an industrial cure profile (ramp of 1°C per minute, followed by a 3-hour isothermal hold at 180°C).

Each of the samples followed the same nomenclature in which the initial functionalization wt.% with APTMOS is the first number, followed by the ratio of APTMOS: G-POSS, then the loading percent into the epoxy/amine system. Each of the sample names and statuses are defined in table 1.

**Table 1:** Sample names and sample status (successful meaning able to be processed into testable materials)

Sample Name	Sample Status
E825+44DDS (Control)	Successful
5%-1:10-1%	Successful
5%-1:10-5%	Successful
5%-1:5-1%	Successful
5%-1:5-5%	Successful
10%-1:10-1%	Successful
10%-1:10-5%	Successful
10%-1:5-1%	Successful
10%-1:5-5%	Gelled in Flask

This resulted in eight formulations total, however only 7 were successful in their preparation. Sample 10%-1:5-5% was unsuccessful in preparation due to premature gelation. This was hypothesized to be due to free primary amines available on the surface of the silica nanoparticles interacting and accelerating the reaction process.

**2.4 Dynamic Mechanical Analysis (DMA) of the epoxy/amine nanocomposite material:**

Dynamic mechanical properties of the cured material, including storage modulus (to determine crosslink density) and tan delta (to determine thermomechanical  $T_g$ ), were measured with a Thermal Analysis Q800 DMA in tensile mode with a strain amplitude of 0.05% and a frequency of 1 Hz. Temperature will be ramped from 35°C to 225°C at a rate of 3°C/minute. Material crosslink density was determined from the equation  $E' = \Phi \nu RT$ ; where  $E'$  is the storage modulus in the rubbery region,  $\Phi$  is the front factor (1),  $R$  is the gas constant (8.314 MPa cm<sup>3</sup>/mol K, and  $T$  is the  $T_g$  of the material plus some consistent shift factor.



## **2.5 Compression testing of the epoxy/amine nanocomposite materials:**

Compression tests was conducted on cylindrical samples with lengths that are approximately 24mm in length and 12mm in diameter. The testing was performed using a MTS Systems Corporation Model 810 servo-hydraulic universal test frame to find the compressive modulus and yield point of the material.

## **2.6 Rheological Testing of the epoxy/amine nanocomposite material:**

Rheology testing was conducted with an ARES G2 rheometer on the uncured material using 25mm parallel plate geometry and an industrial cure profile (prescribed above) starting at 70°C. From 70°C to 125°C, a 20% strain rate was used. From 125°C to 180°C, a 1% strain rate was used. These experiments were conducted to determine the complex viscosity, storage modulus, and loss modulus of the material as it cures.

## **2.7 Scanning Electron Microscopy (SEM) of the epoxy/amine nanocomposite material:**

Materials were gold coated using an Emitech K550x. Sputter coated samples were examined using a FEI Quanta 200 SEM in High Vacuum mode using a voltage of 10kV, to observe particle cell morphology and distribution in the epoxy/amine matrix material.

# **Chapter 3: Results and Discussion**

## **3.1 Dynamic Mechanical Analysis:**

The crosslink density and average molecular weight between crosslinks for each of the samples was determined from the DMA using the equation previously described, and is displayed in table 2.

**Table 2:** Crosslink density and average  $M_w$  between crosslinks

Sample	Avg. $v_e \times 10^{-3}$ (mol/cm <sup>3</sup> )	Standard Deviation $v_e$ $\times 10^{-3}$ (mol/cm <sup>3</sup> )	Avg. $M_c$ (g/mol)	Standard Deviation $M_c$ (g/mol)
Control	4.89	0.01	250.86	0.02
10%-1:10-1%	5.54	0.17	222.44	6.97
10%-1:10-5%	6.10	0.06	202.36	1.96
10%-1:5-1%	6.77	0.01	180.90	0.07
5%-1:10-1%	4.80	0.05	255.09	2.65
5%-1:10-5%	6.35	0.06	194.97	1.74
5%-1:5-1%	5.32	0.08	228.71	3.28
5%-1:5-5%	6.62	0.06	186.80	1.71

It was found that samples ‘10%-1:10-1%’ and ‘10%-1:5-1%’ exhibited higher crosslink densities compared to ‘5%-1:10-1%’ and ‘5%-1:5-1%’ respectively (Table 2).

Nanoparticle surface functionalization with 10wt.% of APTMOS in the first step provide higher amounts of amine functionalities on the surface. This will further allow the nanoparticles to absorb higher amounts of G-POSS on the surface in the second step of the synthetic procedure compared to nanoparticle surface functionalization with 5 wt.% APTMOS. With more G-POSS present on the nanoparticles surface, more epoxide functionalities are present to interact with the epoxy/amine network (i.e. a highly crosslinking site). Therefore, it is considered that, with increased degree of nanoparticle surface modification using G-POSS, the crosslink density of the overall material will increase. For higher loadings of modified nanoparticles in the epoxy/amine system, it was found that ‘5%-1:10-5%’ and ‘10%-1:10-5%’ samples had similar crosslink densities (Table 2). This directly contradicts the prediction that higher functionalization density will increase the overall crosslink density of the material. In addition to that, ‘10%-1:5-1%’ and ‘5%-1:5-1%’ have higher crosslink densities compared to ‘10%-1:10-1%’ and

‘5%-1:10-1%’ respectively. This can be explained as, the higher the amount of epoxide functionalities on the surface imparts steric hindrance effect, which resist all the epoxide functionalities to react with the epoxy/amine network. Since sample 10%-1:10-5% consists of surface modified silica nanoparticles with the largest amount of primary amine functionalization, largest amount of G-POSS modification, and largest level of loading into the epoxy/amine network, it will inadvertently have more steric hindrance. Also, higher nanoparticle loading could also lead to incorporation of more free volume in the system. This free volume can have an effect on the network formation of the overall nanocomposite material. In this case, the large amount of free hole volume is disrupting the formation of the nanocomposite network, resulting in a decreased crosslink density. Therefore, it was concluded that the increased amount of G-POSS on the nanoparticles surface leads to incomplete reaction, and higher loading of functionalized nanoparticles leads to disrupted chain packing and intermolecular interaction throughout the overall matrix. This conclusion holds true for the comparison of sample ‘5%-1:10-5%’ and ‘10%-1:10-5%’ since there is a dramatic increase in the amount of G-POSS in the epoxy/amine network due to increased loading of surface modified silica nanoparticles into the epoxy/amine network. Furthermore, this conclusion explains why the 1:5 G-POSS modification samples exhibit higher crosslink density than that of their 1:10 modification counterparts.

This was further observed from the average molecular weight between crosslinks ( $M_c$ ), which is directly related to the crosslink density of the material. The above explanation holds true for all samples compared in this study.

The glass transition temperature ( $T_g$ ) of each sample was taken from the tan delta peak of DMA analysis and recorded in table 3.

**Table 3:** Glass transition temperatures

Sample	$T_g$ (°C)
Control	198.52
10%-1:10-1%	195.85
10%-1:10-5%	194.25
10%-1:5-1%	208.10
5%-1:10-1%	194.14
5%-1:10-5%	195.87
5%-1:5-1%	191.61
5%-1:5-5%	194.81

It was found that each of the samples, except sample ‘10%-1:5-1%’, exhibited a slightly decreased  $T_g$  than that of the control by a maximum of 6.89°C and a minimum of 2.66°C. Originally, it was hypothesized that with increasing the crosslink density of the material that the  $T_g$  of the material would increase. However, for these samples this is not the case. Therefore, it was determined that the incorporation of nanoparticles disrupt the chain packing of the overall network, which could lead to decrease in  $T_g$ . However, the difference in  $T_g$  is not significant. As for sample ‘10%-1:5-1%’, the  $T_g$  is 9.58°C higher than that of the control network. Since this sample exhibits the highest crosslink density than that of all the other samples, it was determined that the crosslink density of this sample outweighs the effects of the free volume provided with the nanoparticles, giving a higher  $T_g$  than that of the control. Therefore, it was determined that there is a distinct relationship between the free volume of the material and crosslink density and its effects on the  $T_g$  of the material.

### 3.2 Compression analysis of epoxy/amine nanocomposite materials:

Compression analysis was performed to determine the effects that the surface modified silica nanoparticles will have on the modulus, yield stress, and yield strain. The modulus of each sample was determined by taking the initial slope of the stress vs. strain curve that was produced from compressive analysis of the materials. The yield stress and yield strain were determined from the highest point of the “shoulder” of the stress vs. strain curve, also known as the yield point of the material. The values for each testable material were recorded in table 4.

**Table 4:** Average moduli, yield stress, and yield strain

<b>Sample</b>	<b>Average Modulus (MPa)</b>	<b>Average Yield Stress (MPa)</b>	<b>Average Yield Strain (%)</b>
Control	19.82	141.89	12.31
10%-1:10-1%	20.90	146.19	12.37
10%-1:10-5%	21.89	150.54	12.49
10%-1:5-1%	20.25	147.60	13.48
5%-1:10-1%	23.07	147.31	12.77
5%-1:10-5%	23.31	151.56	12.85
5%-1:5-1%	23.17	148.00	12.40
5%-1:5-5%	22.19	150.61	12.82

All networks containing modified nanoparticles exhibited an increase in bulk modulus compared to the control epoxy/amine network. This supports the hypothesis that incorporating the modified silica nanoparticles into the epoxy/amine network increases the modulus of the overall material. It was expected that the highest initial functionalization values, G-POSS surface modification, and loading would allow for the greatest increase in modulus and yield point of the control material. However, this hypothesis was found to be incorrect. As explained earlier, higher numbers of epoxy functionalities on the nanoparticle surface leads to a decrease in crosslinking density due to steric effect. However, more nanoparticles in the system would lead to an increase in

the bulk modulus of the modified networks. Therefore, there is an optimum value at which the silica nanoparticles should be functionalized and surface modified with G-POSS to obtain the greatest possible increase in modulus of the epoxy/amine network.

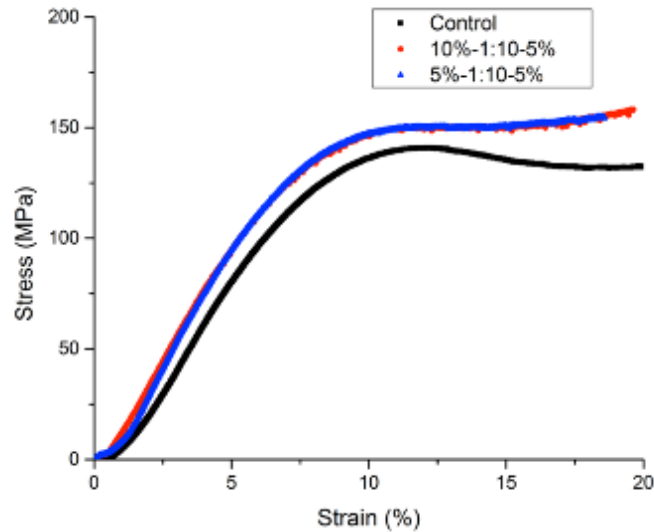


**Figure 4:** General compressive analysis of tested samples to the control

The stress-strain behaviors of ‘10%-1:10-5%’ and ‘5%-1:10-5%’ with respect to the control network is shown in Figure 4, as observed incorporation of G-POSS modified silica nanoparticles also increased the yield stress, the maximum force that the material can withstand before any permanent deformation occurs. It was found that the increase in the yield stress directly correlates to the loading percent into the epoxy/amine network. At each of the lower loaded samples, the yield stress ranges from 146.19 MPa to 148 MPa while the higher loaded samples ranges from 150.54 MPa to 151.56 MPa. Therefore, it was concluded that samples with higher loadings of the surface modified silica nanoparticles would be able to withstand larger amounts of force before permanently deforming, due to the silica nanoparticles being able to disperse the force throughout the entirety of the material. Each of the yield strain values, maximum amount

of deformation that a material can withstand before being permanently deformed, values remained relatively similar to each other, minus that of sample ‘10%-1:5-1%’.

Therefore, it was determined that each of the materials could be deformed to relatively the same extent before permanent damage would occur. As for sample ‘10%-1:5-1%’, the average strain value could be due to multiple competing effects such as high degree of crosslinking and sample inhomogeneity, discussed in section 3.4, as well as noise in the instrument itself. Therefore, no definite conclusion can be made for this value and further experimentation should be conducted.

### 3.3 Rheological Analysis of epoxy/amine nanocomposite materials:

Rheological analysis was performed to determine the effects of nanoparticle surface modification on gel point and viscosity of the material during the cure process previously described. Gel points were determined by the crossover point of the storage and loss moduli. Each of the data profiles follow similar suite to that seen in Figure 5, the storage and loss modulus crossover of sample ‘10%-1:10-5%’.

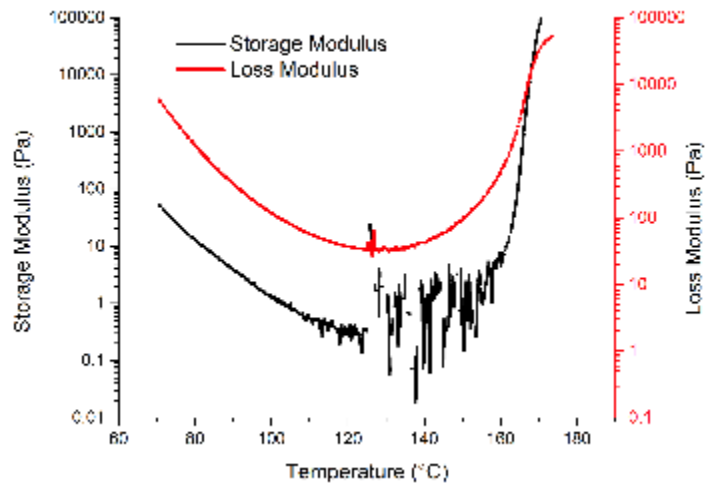


**Figure 5:** Storage and loss modulus crossover of ‘10%-1:10-5%’ during cure process

The noise in Figure 5 is due to the material exhibiting a liquid-like behavior, making it difficult for the instrument to produce a plot at low frequency. Furthermore, the complex viscosity of each sample was recorded and each sample followed similar suit to that of Figure 6, sample 10%-1:10-5%.

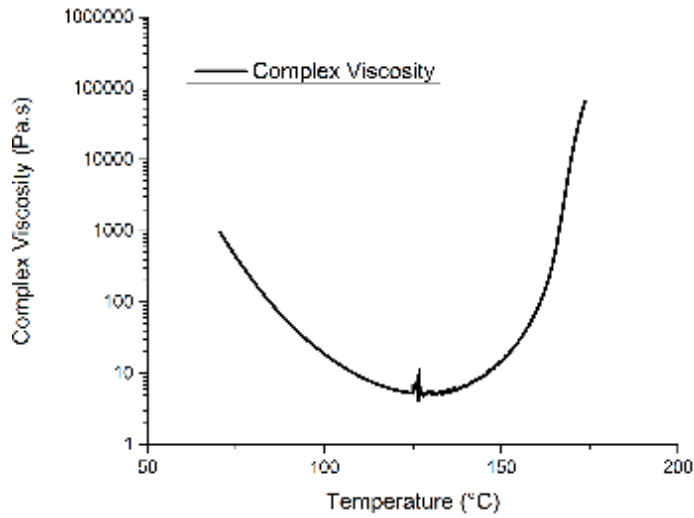


**Figure 6:** Complex viscosity of ‘10%-1:10-5%’ during cure process

The gel point of each material and complex viscosity at 70°C (the initial point of rheological analysis) and 120°C (the onset of the lower viscosity well) were recorded in Table 5.

**Table 5:** Sample gel points, initial viscosities, and lower level viscosities

Sample	Gel Point (°C)	Viscosity at 70°C (Pa*s)	Lower Level Viscosity (Pa*s)
Control	180.00	0.83	0.04
10%-1:10-1%	177.61	2.84	0.12
10%-1:10-5%	168.65	932.41	5.34
10%-1:5-1%	180.00	0.72	0.06
5%-1:10-1%	170.27	344.19	2.32
5%-1:10-5%	178.54	2.15	0.09
5%-1:5-1%	174.53	18.61	0.39
5%-1:5-5%	178.42	2.48	0.12



The gel point of each of the network was found to decrease with the incorporation of the G-POSS modified silica nanoparticles to a maximum of 11.35°C when compared with the gel point of the control (180°C). For samples with initial functionalization densities of 10%, it was determined that higher loadings of the surface modified silica nanoparticles caused the material to gel quicker since sample 10%-1:10-5% gelled at 168.65°C while its lower loading counterparts gelled above 177°C. However, this trend does not hold true for samples with initial functionalization densities of 5%. For samples of this functionalization density, the opposite trend is found in that samples with lower loadings gelled faster than samples with higher loadings. In this case, sample 5%-1:10-1% gels the fastest at 170.27°C. Each of the gel temperatures correlates to the initial complex viscosity value at 70°C. It was found that higher initial complex viscosity values caused earlier gel temperatures. In which case, sample 10%-1:10-5% exhibited the highest initial viscosity, 932.41 Pa\*s, and the earliest gel temperature, 168.65°C, while sample 10%-1:5-1% exhibited the lowest initial viscosity, 0.72 Pa\*s, and the highest gel temperature, 180°C.

As observed, the gel points vary depending on the functionalization density and the loading of the surface modified silica nanoparticles. It is now hypothesized that there is a trending curvature that can be formulated to correlate these variable to help predict the gel point of the material. Therefore, further experimentation must be conducted to investigate this possibility.

#### **3.4 Scanning Electron Microscopy of the Epoxy/amine Nanocomposite Materials:**

Scanning electron microscopy (SEM) was performed on each of the nanocomposite materials to observe the morphology and dispersion of the surface modified silica nanoparticles after the completion of the cure phase.

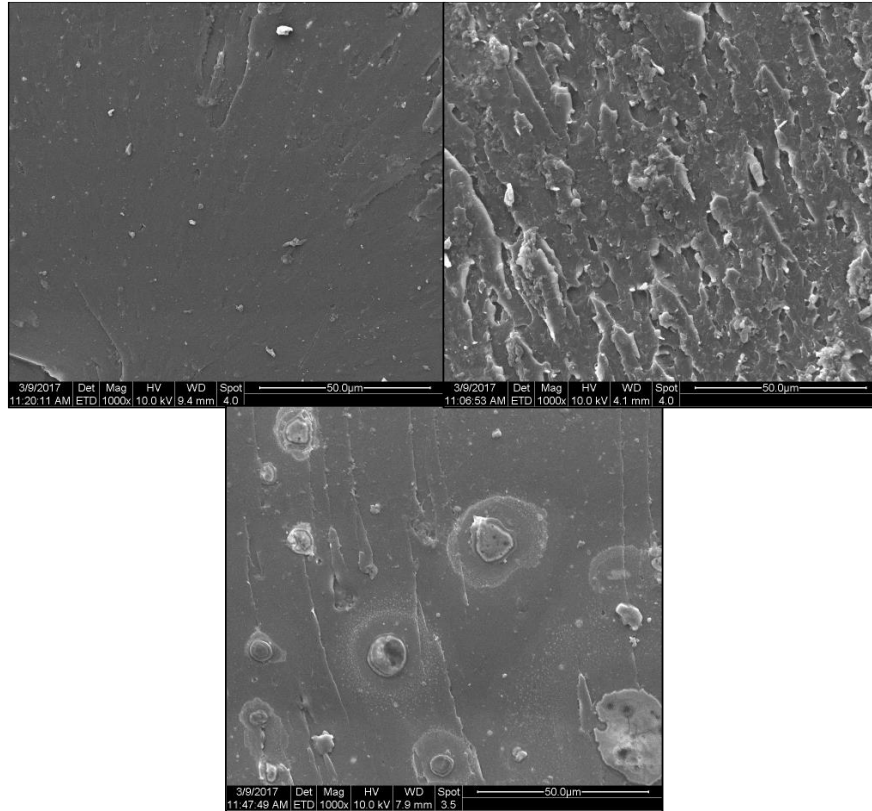


**Figure 7:** sample ‘10%-1:10-1%’ (top left), sample ‘10%-1:10-5%’ (top right), sample ‘10%-1:5-1%’ (bottom)

The SEM micrographs in Figure 7 were taken at 1000x magnification of the fractured surface. Samples ‘10%-1:10-1%’ and ‘10%-1:10-5%’ showed no clear evidence of aggregation of the surface modified silica nanoparticles in the bulk of the material.

However, sample ‘10%-1:5-1%’ exhibited large amounts nanoparticle aggregation during the curing phase of the material.

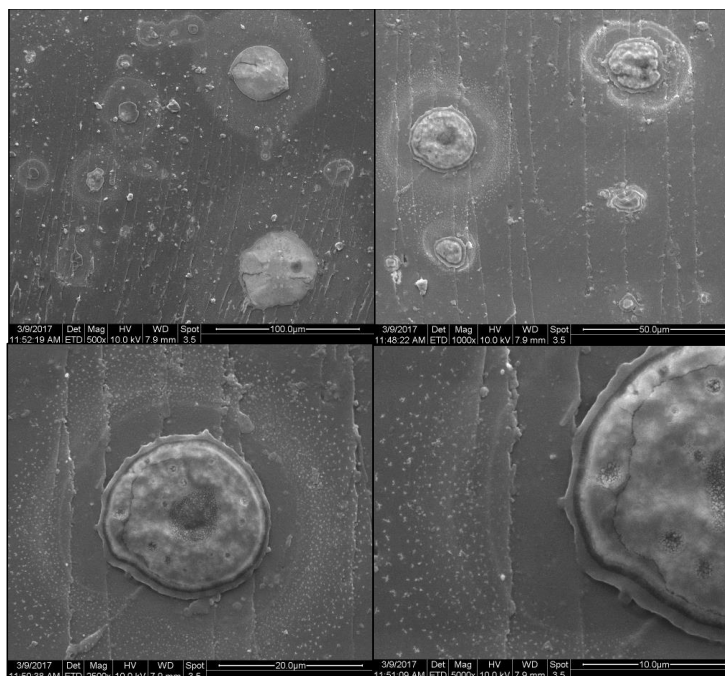


**Figure 8:** sample ‘10%-1:5-1%’ at 500x (top left), 1000x (top right), 2500x (bottom left), and 5000x (bottom right) magnification

Figure 8 shows the aggregation of the G-POSS modified silica nanoparticles in sample ‘10%-1:5-1%’ in the bulk of the material. The aggregation is expected to be due to the surface modification of the silica nanoparticle and their ability to aggregate during the curing phase, since the solution was clear in the flask during material preparation. Since this sample was made with the higher amine functionalization density and at the lowest G-POSS modification value (1:5) there is the possibility of unreacted primary amines that are still present on the surface of the silica nanoparticle. Therefore, these particles have the ability to react with each other and increase in size during the surface modification step (G-POSS) in the procedure. Furthermore, since silica nanoparticles have a tendency to aggregate during the cure phase when the viscosity of the material is at its minimum, the particles will be more likely to aggregate. However, sample ‘10%-1:5-5%’ would need to have been successfully prepared to further prove this claim.

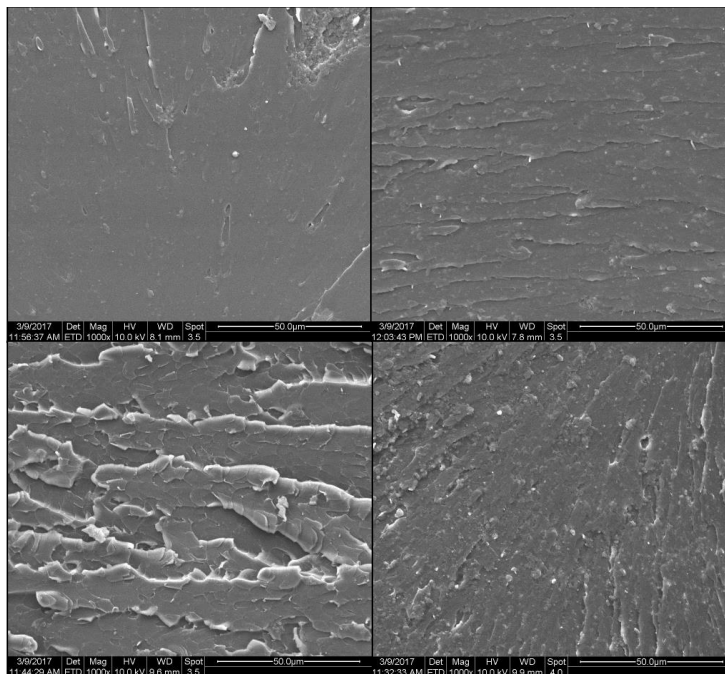


**Figure 9:** sample ‘5%-1:10-1%’ (top left), sample ‘5%-1:10-5%’ (top right), sample ‘5%-1:5-1%’ (bottom left), and sample ‘5%-1:5-5%’ (bottom right)

The images in Figure 9 show the samples with the incorporation of silica nanoparticles with the incorporation of silica nanoparticles made with an initial functionalization density of 5% by weight at a magnification of 1000x, each image being in taken of the bulk of the material. These images are similar to those taken of samples ‘10%-1:10-1%’ and ‘10%-1:10-5%’ in that no obvious forms of nanoparticle aggregation can be seen. Therefore, the dispersion of these nanoparticles is better within the bulk of the material than that of sample ‘10%-1:5-1%’. This was also observed in material preparation since the solution was clear during the homogenizing of the material.

#### Chapter 4: Conclusions

The thermomechanical properties of the epoxy/amine networks with the incorporation of G-POSS modified silica nanoparticles strongly depends on the network formation (chain packing, intermolecular interaction, crosslink density, and free volume

present in the network) with respect to surface modification of nanoparticles and loading level of modified nanoparticles. It was found that incorporating nanoparticles with higher amine modification values would increase the crosslink density of the resulting material due to increased functionalization of the nanoparticle (i.e. a highly crosslinking site). It was also found that introducing more surface modified nanoparticles into the system would further increase the crosslink density of the material due to more highly crosslinking site present within the system. Furthermore, high amounts of G-POSS modification caused a lessened crosslink density to as compared to that of its lower G-POSS modification counterpart. This was determined to be due to the steric effects disrupting network formation and chain stacking, and incorporation of more free volume in the system. By incorporating the surface modified silica nanoparticles into the epoxy/amine network, the modulus of the epoxy/amine network is increased. It was further determined that amine functionalization values, G-POSS modification values, and percent loading into the epoxy/amine network all played a role into the extent to which the modulus would be increased. Therefore, there is an optimal value to which the surface modification and loading will give the greatest increase in the modulus of the material. Furthermore, it was determined that the yield stress of the material was also increased with the loading of the surface modified silica nanoparticles, in which case at higher loadings of all types of modified silica nanoparticles would offer the highest yield stress. The kinetics of the reaction also depends on the amine functionalization density and the loading of silica nanoparticles into the system. At higher amine functionalization densities, the material gels at faster higher loadings. At lower amine functionalization densities, the material gels faster at lower loadings. In each formulation, except '10%-

1:5-1%', dispersed fairly well into the epoxy/amine network so that no aggregation of the silica nanoparticles were distinctly visible at 1000x magnification within the bulk of the material. However, sample '10%-1:5-1%' exhibited large aggregation of silica nanoparticles within the bulk of the material. The aggregation of the nanoparticles is expected to be due to the nanoparticles reacting with one another to form large aggregated particles. These large aggregations could be the reason for the rise in the  $T_g$  of this particular sample. Since there are large aggregates of nanoparticles within the bulk of the material (sample inhomogeneity), it is expected that there is lessened disruption of network formation and chain stacking due to the free volume of the POSS cage playing less of a factor. Therefore, the idea that the value of the crosslink density of this particular sample outweighs the value free volume, with respect to their effects on the samples  $T_g$ , is strengthened. However, no definite conclusion can be made regarding this aspect without the comparison to sample 10%-1:5-5% (gelled in flask).

### **Chapter 5: Future Work**

In future research, experiments should be conducted to investigate the properties of epoxy/amine networks containing G-POSS surface modified silica nanoparticles under optimal nanoparticle modification values and loading levels. Based on the data presented, optimal nanoparticle modification levels can be determined by the use of a design of experiment (DOE). This would allow for optimal properties of the nanocomposite materials to be achieved.

Furthermore, experiments should be conducted to investigate the effects of silica nanoparticle surface modification with differing types of POSS based on their reactive functionalities, such as epoxyhexyl and octadecyltrimethylsilyl POSS, and study

the effects on the mechanical and rheological properties of epoxy/amine networks. As well as using different types of POSS molecules, the use of different epoxy resins and curatives should also be investigated. Furthermore, an investigation of different cure profiles and the effects they will have on the material's properties should also be conducted.

## References:

- (1) Why Composites? <http://www.premix.com/why-composites/adv-composites.php>  
(accessed Mar 20, 2016).
- (2) Wang, R.; Zheng, S.; Zheng, P. Introduction to polymer matrix composites.  
*Polymer matrix composites and technology*; pp 1-24
- (3) Thermoset vs. Thermoplastics. <http://modorplastics.com/thermoset-vs-thermoplastics> (accessed Mar 20, 2016)
- (4) Odian, G. *Principles of Polymerization*, Fourth Edition, Wiley-Interscience, 2004.
- (5) Carey, F. *Organic Chemistry*, Fourth Edition, McGraw-Hill, 2000.
- (6) Prime, R. B. An Introduction to Thermosets. <http://www.primethermosets.com>  
(accessed Mar 20, 2016)
- (7) Winter, H. H. *Polym. Eng. Sci.* **1987**, 27, 1698-1702
- (8) Zhao, C.; Zhang, G.; Zhao L. *Molecules* **2012**, 17, 8587-8594
- (9) Sprenger, S. *J. Appl. Polym. Sci.* **2013**, 1421-1428
- (10) Ding, Z.; Grimmond, B.; Luttrell, M.; Rubinsztajn, S.; DeMoulpied, D.; Blohm, M. Chelator-Functionalized Nanoparticles. U.S. Patent 20090087381, April 3, 2012
- (11) Luechinger, M.; Prins, R.; Pirngruber, G. D. *Microporous Mesoporous Mater.* **2005**, 85, 111-118
- (12) Schwab, J. J.; Lichtenhan, J. D. *Appl. Organometal. Chem.* **1998**, 12, 707-713
- (13) Ayandele, E.; Sarkar, B.; Alexandridis, P. *Nanomaterials* **2012**, 2, 445-475
- (14) Jiao, J.; Wang, L; Lv, P.; Cui, Y.; Miao, J. *Mater. Lett.* **2014**, 129, 16-19



- (15) Kwan, K. The Role of Penetrant Structure on the Transport and Mechanical Properties of a Thermoset Adhesive. Ph.D. Dissertation, Virginia Polytechnic Institute and State University, July 1998
- (16) Tension and Compression Testing. <http://www.mee-inc.com/hamm/tension-and-compression-testing/> (accessed Mar 20, 2016).
- (17) Electron microscopy (EM) <http://www.vcbio.science.ru.nl/en/image-gallery/electron/> (accessed Mar 20, 2016).
- (18) Scanning Electron Microscopy (SEM) Imaging <https://www.dsimagingllc.com/scanning-electron-microscopy-imaging-and-analysis/#hi> (accessed Mar 20, 2016).